in many applications the large depth of field in SEM images (typically at least 100 times greater than for a comparable optical microscope) is more relevant than high resolution. An important factor in the success of the SEM is that images of three-dimensional objects are usually amenable to immediate intuitive interpretation by the observer. The range of applications of SEM can be extended by adding other types of detector, e.g. for light emission caused by electron bombardment, or cathodoluminescence (CL).

1.2.1 Use of SEM for analysis

Scanning electron microscopes commonly have an X-ray spectrometer attached, enabling the characteristic X-rays of a selected element to be used to produce an image. Also, with a stationary beam, point analyses can be obtained, as in EMPA. (The spatial resolution with respect to analysis is, however, still limited to about 1 μm by beam spreading, despite the higher resolution obtainable in scanning images.) Since EMP instruments have electron imaging facilities, used primarily for locating points for analysis, the functions of the two instruments overlap considerably. The SEM is optimised for imaging, with analysis as an extra, whereas in the EMP the priorities are reversed and various additional features that facilitate analysis are incorporated.

1.3 Geological applications of SEM and EMPA

The advantages of the SEM as an imaging instrument (high spatial resolution, large depth of field, and simple specimen preparation) make it an invaluable tool in the following branches of geology.

Palaeontology. The SEM is ideally suited to the study of fossil morphology, especially that of micro-fossils.

Sedimentology. Three-dimensional images of individual sediment grains and inter-growths can be obtained; data on fabric and porosity can also be generated.

Mineralogy. The SEM is very effective for studying crystal morphology on a micro-scale.

Petrology. The ability to produce images of polished sections showing differences in mean atomic number is very useful both in sedimentary and in igneous petrology.

The reasons for the widespread application of EMPA to geology (whether carried out in a 'true' EMP instrument or SEM with X-ray spectrometer fitted), especially in the fields of mineralogy and petrology, can be summarised as follows.

(1) Specimen preparation is straightforward and entails the use of existing techniques of section-making and polishing with only minor modifications.
(2) The technique is non-destructive, unlike most other analytical techniques.
(3) Quantitative elemental analysis with accuracy in the region of ±1% (for major elements) can be obtained.
(4) All elements above atomic number 3 can be determined (with somewhat varying accuracy and sensitivity).
(5) Detection limits are low enough to enable minor and trace elements to be determined in many cases.
(6) The time per analysis is reasonably short (usually between 1 and 5 min).
(7) Spatial resolution of the order of 1 μm enables most features of interest to be resolved.
(8) Individual mineral grains can be analysed *in situ*, with their textural relationships undisturbed.
(9) A high specimen throughput rate is possible, the time required for changing specimens being quite short.

These characteristics have proved useful in the following subject areas.

Descriptive petrology. The EMPA technique is commonly used for the petrological description and classification of rocks and has an importance comparable to that of the polarising microscope.

Mineral identification. As an adjunct to polarised-light microscopy and X-ray diffraction, EMPA provides compositional information that assists in mineral identification.

Experimental petrology. For experimental studies on phase relationships and elemental partitioning between coexisting phases, the spatial resolution of the electron microprobe is especially useful, given the typically small grain size.

Geothermobarometry. The EMPA technique is ideally suited to the determination of the composition of coexisting phases in rocks, from which temperatures and pressures of formation can be derived.

Age determination. Th–U–Pb dating of minerals containing insignificant amounts of non-radiogenic Pb (such as monazite) is possible by EMPA, with higher spatial resolution than can be obtained with isotopic methods, though lower accuracy.

Zoning. The high spatial resolution of the technique enables zoning within mineral grains to be studied in detail.

Diffusion studies. Experimental diffusion profiles in geologically relevant systems can be determined with the electron microprobe, its high spatial resolution being crucial in this field.

Modal analysis. Volume fractions of minerals and other data can be obtained by automated modal analysis, mineral identification being based on X-ray and sometimes backscattered-electron signals.

Rare-phase location. Grains of rare phases can be located by automated search procedures, using the X-ray signal for one or more diagnostic elements.

Compound %

Sample	Na2O	SiO2	MgO	Al2O3	SO2	K2O	CaO	Cl	TiO2	Cr2O3	MnO	NiO	FeO	ZrO2	HfO2	BaO	Total
#1	0.337	43.562	0.478	29.023	0.014	10.835	0	0.009	0.182	0.026	0.279	0.004	5.314	0.048	11.6	0.011	90.101
#2	0.275	43.391	0.499	29.129	0.028	10.8	0	0.017	0.175	0	0.275	0.043	5.25	0.093	13.3	0.026	89.979
#3	0.311	41.765	0.428	29.241	0.062	10.688	0	0	0.15	0.004	0.272	0.033	5.179	0.023	11.5	0.023	88.273
#4	0.28	42.486	0.426	29.556	0	10.799	0.386	0	0.19	0.004	0.001	0.003	4.943	0.037	10.3	0.039	89.05
#5	11.687	66.087	0	18.989	0.043	0.105	0	0.006	0.017	0	0.322	0.01	0.087	0	10.8	0.023	97.432
#6	0.985	42.935	0.05	34.987	0.014	9.869	0	0	0.107	0	0.192	0	0.531	0.053	11.3	0	89.959
#7	0.774	35.3	0.191	27.491	0.02	7.713	0	0.019	0.043	0	0.297	0.048	0.798	0.047	11.3	0.026	72.676
#8	1.074	43.695	0.275	33.571	0.008	9.896	0	0.004	0.322	0	0.243	0.042	1.021	0.016	10.4	0.018	90.008
#9	1.134	42.722	0.277	33.397	0.014	9.638	0	0.105	0.001	0	0.178	0.023	0.847	0.057	11.5	0.01	88.506
#10	1.179	42.681	0.035	35.948	0	9.608	0	0.025	0.012	0	0.132	0.006	0.208	0.058	9.3	0.057	89.311
#11	0.91	40.642	0.012	35.158	0	8.53	0.2	0.013	0.025	0.012	0.378	0	0.289	0.123	9.3	0.016	90.013
#12	1.047	38.387	0.138	34.711	0.002	8.342	0.203	0.011	0.13	0.025	0.179	0.008	0.174	0.058	12	0.047	88.625
#13	1.095	38.706	0.118	34.66	0.014	8.288	0.222	0.021	0.007	0.009	0.178	0.017	0.165	0.066	10.1	0.032	83.625
#14	1.224	42.711	0.126	35.247	0.02	9.488	0	0.02	0.022	0.028	0.138	0	0.217	0.066	10.1	0.004	83.461
#15	1.163	41.823	0.05	34.558	0.028	9.57	0.014	0.002	0.038	0	0.063	0	0.18	0.058	10.8	0.002	86.177
#16	0.198	43.004	0.035	19.756	0	9.831	0.007	0.017	0.118	0.031	3.063	0.008	2.518	0.032	11.3	0.003	87.565
#17	0.26	42.386	0.058	20.321	0	9.757	0.003	0.013	0.122	0.009	2.966	0.018	2.375	0.004	—	0.001	78.309
#18	0.26	40.576	0.058	20.138	0.02	9.811	0	0.011	0.085	0.009	3.223	0.022	2.581	0.002	0.04	0	78.553
#19	0.295	41.453	0.038	19.858	0.03	9.697	0	0.021	0.067	0.004	3.258	0.006	2.542	0.045	0.081	0.009	76.813
#20	0.236	41.453	0.046	19.595	0.002	9.657	0	0.002	0.028	0.029	3.063	0.001	2.551	0.01	0.131	0.026	77.412
#21	0.565	41.436	0.051	32.447	0.04	9.744	0	0.02	0.033	0.047	2.764	0	0.226	0.032	0.07	0.009	76.791
#22	0.542	41.609	0.041	32.349	0.022	9.878	0	0.012	0.042	0.012	0.808	0	0.201	0.066	0.05	0.026	85.389
#23	0.566	40.706	0	32.85	0.008	9.885	0	0.017	0.042	0.009	0.713	0	0.148	0	0.037	0.018	85.559
#24	0.597	40.587	0	33.207	0	9.805	0	0	0.048	0.009	0.59	0	0.142	0	0.05	—	85.021
#25	0.616	40.379	0.01	32.702	0	9.567	0	0	0.037	0.009	0.693	0	0.118	0	0.106	—	84.255

(top block)

Sample	Na2O	SiO2	MgO	Al2O3	SO2	K2O	...	MnO	NiO	FeO	ZrO2	HfO2	BaO	Total ←	Total
#19	0.239	19.246	0.027	11.257	0.009	5.937		1.295	0.004	5.314	0.048	11.6	0.007	60.909	100
#20	0.269	19.494	0.041	11.006	0.017	5.817		1.298	0.002	1	0.009		0	60.979	100.001
#21	0.217	19.637	0.032	10.94	0.001	5.836		1.229	0	1.011			0.001	61.058	100
#22	0.452	17.102	0.032	15.783	0.015	5.13		0.267	0	0.078			0.004	61.118	99.999
#23	0.433	17.142	0.025	15.707	0.009	5.191		0.282	0	0.069			0	61.1	100
#24	0.455	16.88	0	16.054	0.003	5.229		0.25	0	0.051	0.006		0.003	61.038	99.998
#25	0.48	16.806	0	16.206	0.009	5.18		0.207	0	0.049	0.004			61.05	100
	0.5	16.881	0.006	16.113	0	5.102		0.246	0	0.041	0.013			61.081	100

Peak c/s

Sample	Na	Si	Mg	Al	S	K	Ca	Cl	Ti	Cr	Mn	Ni	Fe	Zr	Hf	Ba	O
#1	28	6724.4	77.2	5329.3	2.5	1739.4	15.4	4	53.5	5	23.1	10.9	365.2	1.2	11.6	22.9	N/A
#2	23.8	6689.5	79.8	5363	2.5	1734.7	15.2	4.3	49.6	5.6	21	10.1	362.9	1.2	13.3	24.7	N/A
#3	27.5	6405.4	68.4	5371	2.6	1718	14.8	3.4	56.5	5.3	21.9	11.2	355.1	2.1	11.5	25.9	N/A
#4	25.6	6526	72.1	5442.1	3.2	1734	14.2	4.3	48.7	4.8	21.7	10.5	338.5	1.6	10.3	22.8	N/A
#5	956.7	10726	10.7	3384.2	2.7	25.2	64	3.5	22.8	4.6	5.9	9.2	10.6	1.5	10.8	25	N/A
#6	82.1	6493.9	23.1	6666.3	2.1	1566.5	11.3	2.9	28.6	4	23.2	9.6	44	2.7	11.3	27.4	N/A
#7	63.3	5261.3	38.9	5152.5	2.3	1223.3	14.3	3.1	38.4	4.2	15.7	8.1	57.8	1.9	11.3	21.3	N/A
#8	87.1	6648.2	52.7	6362.8	2.3	1574.2	14.3	3.1	38.1	4.6	22	9.3	74.7	1.4	10.4	26.3	N/A
#9	93.5	6362.8	51.9	6321.3	2.9	1530.8	13.3	3.9	40.7	4.3	17.2	9.3	65	1.7	11.5	21.9	N/A
#10	97.6	6869.5	19.8	6869.5	2.8	1526.3	13.2	4.2	24	4.1	11.9	9.4	26.3	1.6	9.3	20.6	N/A
#11	77.6	6052.1	14.9	6702.6	2.3	1353.5	13.3	5.3	22.7	2.8	27.5	8.5	17.4	1.3	9.3	23.2	N/A
#12	90.2	5673	32.2	6595.3	2.9	1322.7	41.2	4.2	24.2	4.7	14.7	10.6	20.7	2.4	12	22	N/A
#13	91.8	5723.1	31.6	6579.7	3.3	1313.2	43.9	2.8	24.3	3.8	14.4	9.7	20.7	1.3	10.1	22	N/A
#14	101.7	6418.6	31.5	6719.1	2.1	1506	41.6	2.4	24.7	5	15.6	9.5	19.6	2.2	9.1	22	N/A
#15	95.8	6286.4	22.2	6593.3	2.4	1518.7	15.6	3.5	26	3.5	13.9	9.9	19.8	1.5	11.3	21.1	N/A

Total ←— volatile K2O x
H2O
F
organic carbon

No. 1 Yeonhwa

No. 2 Yeonhwa

Ulchin

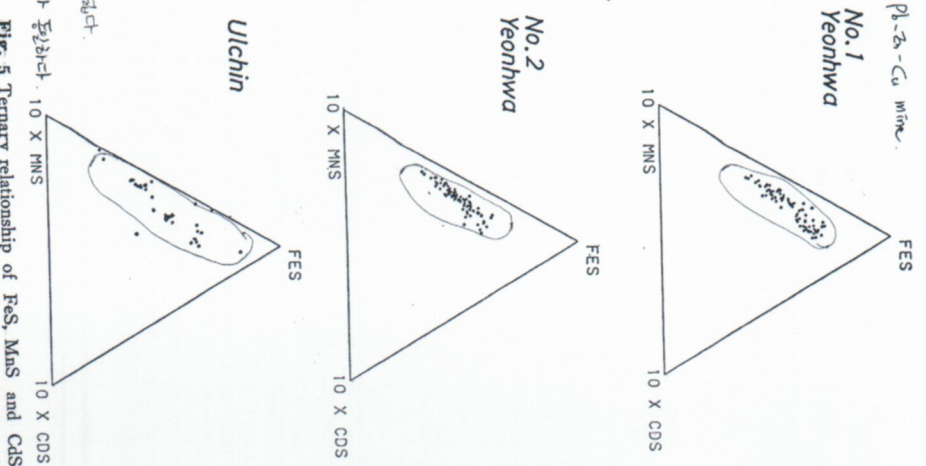*(Ternary diagrams with axes: 10 X MNS, FES, 10 X CDS)*

Fig. 5 Ternary relationship of FeS, MnS and CdS contents in sphalerites from the No. 1 and the No. 2 Yeonhwa and the Ulchin mines.

Compositional variation of sphalerites (regional scale)

A total of 42 metallic mines comprising W-(Mo-Bi), Cu-(Pb-Zn), Zn-Pb-(Cu), Fe, Ag and Au mines were concerned in regional scale to determine the variation of Fe, Mn and Cd contents in sphalerites.

Interrelation of mean FeS and MnS contents in sphalerites is plotted in Figure 6. In general, the FeS contents seem to be proportional to the

MnS contents. The relationship between mean CdS and MnS contents is shown in Figure 7. Dotted line in Figure 7 means the average value of CdS mole % in sphalerites (up to 0.5 mole %) from hydrothermal metallic ore deposits (Mookherjee, 1962; Shimazaki & Shimizu, 1980). Most of Cu-(Pb-Zn), Zn-Pb-(Cu), and Fe deposits are characterized by low CdS contents in sphalerites (less than 0.5 mole %). Most of tungsten deposits and some gold deposits (Samgwang, Gubong, and Gyeolseong Au mine) have high CdS contents in sphalerite (more than 0.5 mole %). Tungsten deposits include Daewha, Sangdong, Susan, Weolak, Ilgwang, and Garisan mines. The MnS contents in sphalerites show two modes of distribution: one is relatively high MnS (more than 1.0 MnS mole %) and the other is low MnS (less than 1.0 mole %). It is noteworthy that sphalerites from Zn-Pb-(Cu) deposits contain variable amounts of manganese ranging from 0.05 mole % (Sambo mine) to 4.53 mole % (Janggun mine). Compared with other mines, MnS contents in sphalerites from Janggun, Ulchin, Sinyemi, No. 1 Yeonhwa, No. 2 Yeonhwa and Youngwug Zn-Pb mines have high range more than 1.0 mole %. Such results correspond to the abundance of manganese minerals in orebodies or skarns of these deposits.
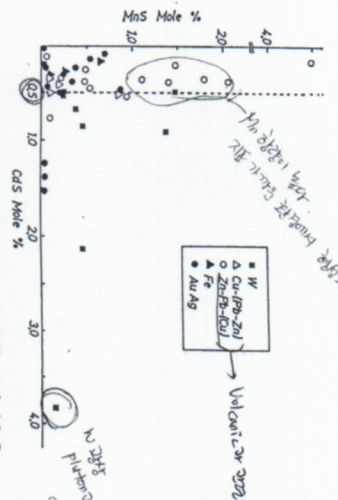
(Scatter plot: FeS Mole % vs MnS Mole %; legend: ■ W, △ Cu-(Pb-Zn), ○ Zn-Pb-(Cu), ▲ Fe, ● Au Ag)

Fig. 6 The relation between mean MnS and FeS contents in sphalerites collected from 42 various metallic ore deposits.

(Scatter plot: MnS Mole % vs CdS Mole %; legend: ■ W, △ Cu-(Pb-Zn), ○ Zn-Pb-(Cu), ▲ Fe, ● Au Ag)

Fig. 7 The relation between mean CdS and MnS contents in sphalerites collected from 42 various metallic ore deposits. Dotted line means the average value of CdS mole % in sphalerites ($\sim$0.5 mole %) suggested by Mookherjee (1962), and Shimazaki and Shimizu (1980).

All of Cu, Fe, Au, Ag, and W deposits are characteristic in low MnS contents except two W deposits such as Susan and Cheongyang mines. Ternary relationship of FeS-MnS-CdS contents in sphalerites is plotted in Figure 8. As discussed above, sphalerites from Cu-(Pb-Zn), Zn-Pb-(Cu), and Fe deposits are relatively depleted in cadmium, whereas sphalerites from W and some Au mines are enriched in Cd. CdS MnS contents are relatively variable in sphalerites from base metal deposits.
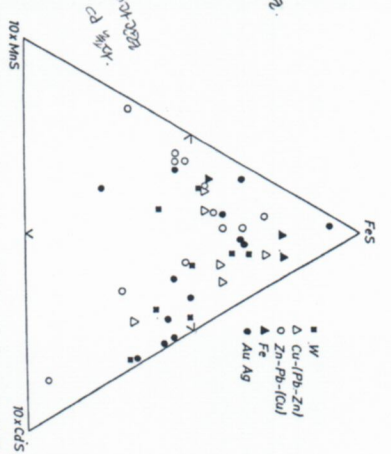
Considering the related igneous rocks of the studied ore deposits, low Mn contents in sphalerites seem to be associated with plutonic igneous activity, and low Cd contents tend to be associated with hypabyssal to effusive activity (Figure 9). But Cd contents in sphalerites from the studied ore deposits which are geologically associated with plutonic activity are highly variable.

Source of cadmium in sphalerites

Cadmium contents in sphalerites occurring in W ore deposits are exceptionally high, ranging up to 3.83 mole % CdS in the Daewha mine.
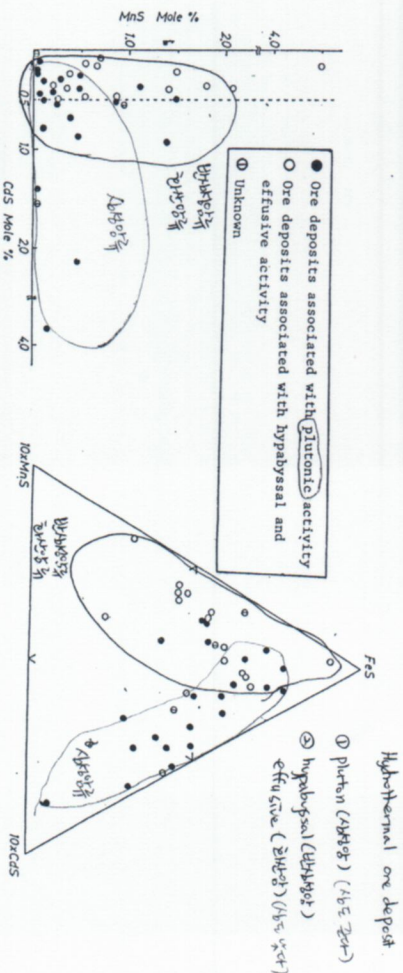
(Ternary diagram with axes: 10xMnS, FeS, 10xCdS; legend: ■ W, △ Cu-(Pb-Zn), ○ Zn-Pb-(Cu), ▲ Fe, ● Au Ag)

Fig. 8 Ternary relationship of FeS, MnS, and CdS contents in sphalerites from 42 various metallic ore deposits.

(Plots: MnS Mole % vs CdS Mole %, and ternary 10xMnS, FeS, 10xCdS)

Legend:
● Ore deposits associated with plutonic activity
○ Ore deposits associated with hypabyssal and effusive activity
⊕ Unknown

Fig. 9 The relationship of CdS-MnS, and FeS-MnS-CdS contents in sphalerites with reference to the related igneous rocks of the studied 42 ore deposits.

$$* \quad Zn^{2+}_{aq} + Cd_{sp} \rightleftharpoons Cd^{2+}_{aq} + Zn_{sp}$$

aq : aqueous solution
sp : sphalerite

$$k = \left(\frac{a_{Cd^{2+}} \cdot a_{Zn}}{a_{Zn^{2+}} \cdot a_{Cd}} \right)_{sp}$$

$$\therefore \left(\frac{a_{Cd}}{a_{Zn}} \right)_{sp} = \frac{1}{k} \cdot \left(\frac{a_{Cd^{2+}}}{a_{Zn^{2+}}} \right)_{aq}$$

⇒ aq 중의 Cd 농도에 좌우된다.

sphalerite 내 Cd 농도

Sphalerite 중
Cd의 상대적 저농도는 왜?

$$(Zn, Fe, Mn, Cd, \cdots) S$$

Compositional Variation of Sphalerites from Some Hydrothermal Metallic Ore Deposits in the Republic of Korea*

Hyo Tack CHON**, Hidehiko SHIMAZAKI*** and Kohei SATO****

Abstract: FeS, MnS and CdS contents of sphalerites from fourteen Korean hydrothermal deposits, are measured by an electron probe microanalyzer. The results are summarized in Table 2. Relatively MnS-rich sphalerites are found in the deposits where sphalerites are enriched in FeS molecule. Sphalerites from Zn-Pb deposits are characterized by high MnS and low CdS contents. Sphalerites from W deposits are high in CdS contents but those from Cu and/or Fe deposits are low in MnS and CdS contents.

Introduction

Sphalerite is one of the commonest ore minerals occurring in hydrothermal metallic ore deposits. Descriptions of composition of sphalerite from various parts of the world are found in so many literatures. Electron probe microanalysis has been established to be a useful technique for the determination of major and minor element contents in sphalerite since classical works (e.g. WILLIAMS, 1967). FeS content in sphalerite has been proposed as a sensitive indicator for sulfur fugacities prevailed during the ore precipitation (BARTON and TOULMIN, 1966). The FeS content in sphalerite is also useful as geobarometer when sphalerite coexists with hexagonal pyrrhotite and pyrite (e.g. SCORR and BARNES, 1971).

The data of sphalerite composition have been included in so many papers discussing the genesis of individual ore deposits, but only few papers have attempted to clarify the compositional variation of sphalerite from the regional viewpoint. One of the most comprehensive, classical reviews on the minor element contents in sphalerite was carried out by FLEISCHER (1955). In Japan, TAKAHASHI (1963) analyzed 366 specimens of sphalerite from the Inner zone of Northeast Japan (so-called Green Tuff region) by a spectroscopy method, to show the regional characteristics and geochemical behavior of trace elements in view of the type of ore deposits and their condition of ore formation. SHIMAZAKI and SIMIZU (1980) showed that FeS, MnS and CdS contents in sphalerites from several tens of skarn-type deposits in Japan represent certain regularities, and gave possible genetical implications of these regularities.

In Korea, SO (1977) studied the trace element geochemistry of sphalerites collected from 16 Zn-Pb deposits of various geologic settings, and concluded that specific correlations of the trace elements are controlled by geological settings and by physicochemical conditions of the ore formation. His conclusion was unfortunately confined to sphalerites from Zn-Pb deposits. Until now in Korea, therefore, there have been no systematic studies on the compositional variation of major and minor elements in sphalerites in relation to their associated metallic elements

Table 1 Brief descriptions of geology and ore deposits of the 14 studied mines.

No.	Name of mine	Type of ore deposits	Major metallic minerals	By-products	Wall rocks	Age of wall rocks	Related igneous rocks	Age of igneous rocks	Remarks
1	Buyong	veins (net-works)	Ag, Pb		rhyolite	late Jura.-Cret.	granite (?)	Cret.	operating
2	Sihung	skarn	Pb, Zn, Cu		lime-silicates	Pre-Cam.	felsite (?)	Cret.	closed
3	Sinyemi Eastern D.	lens or pipe	Zn, Pb	Mo, Cu, W	limestone	Cam.	felsite porphyry liparite	Cret.	operating
	Western D.	skarn	Zn, Mo, Cu	W	limestone	Cam.	felsite liparite	Cret.	
4	Sangdong	skarn	W, Bi, Mo	Au	calcareous shale	Cam.	?		operating
5	Geodo	skarn	Fe, Cu	Au	limestone limestone porphyry	Cam. Cret.	diorite porphyry	Cret.	operating
6	No. 1 Yeonhwa	skarn	Zn, Pb	Ag	limestone	Cam.	quartz porphyry	Cret.	operating
7	No. 2 Yeonhwa	skarn	Zn, Pb	Cu, Ag	limestone	Cam.	granite porphyry	Cret.	operating
8	Ulchin	skarn	Cu		limestone	Cam.	liparite	Cret.	developing
9	Susan	veins	W, Mn	Mo	granite	Cret.	granite	Cret.	closed
10	Wolag Kwangchon D.	veins	Cu	Pb, Zn, Cu	hornfels granite	Ordo. Cret.	granite	Cret.	operating
	Dongan D.	veins	W, Mo	Pb, Zn, Cu	lime-silicates hornfels	Ordo.	granite	Cret.	
11	Ulsan	skarn	Fe		granite limestone hornfels	Cret.	granite (?)	Cret. (?)	operating
12	Ilgwang	breccia pipe	Cu, W	Ag	granite diorite	Cam. (?)	grano-diorite	Cret.	operating
13	Mulgum	veins	Fe		andesite	Cret.	granite (?)	Cret. (?)	operating
14	Haman	veins	Cu	Co, Ag, Au	grano-diorite hornfels	Cret.	grano-diorite	Cret.	closed

and geologic environments of the deposits.

In the present paper, sphalerites taken from 14 representative mines in Korea, were partially analyzed for iron, manganse and cadmium by using an electron probe microanalyzer. Compositional variation of the sphalerites is given with brief descriptions of their occurrences, and will be compared from the regional viewpoint.

Sample Preparation and Analytical Procedure

Brief descriptions on geology and ore deposits of the studied 14 mines are listed in Table 1. The age of the related igneous activities is mainly based on the present authors'

recent consideration on the metallogeny in Korea (Shimazaki et al., 1981a),: A locality map of the studied mines, and mineral assemblages found in them are given in a separate paper (Shimazaki et al., 1981b).

Three kinds of polished sections were prepared for the present study of electron probe microanalyses. The first one is made from mill products (concentrates) collected from the mineral dressing plant of the studied mines, because mill products are thought to be representative mixture of ore minerals in the deposits. As shown in Table 2, analytical results of the Buyong (Ag-Pb), No. 1 and No. 2 Yeonhwa (Zn-Pb), Ulchin (Zn-Pb) and Ulsan

Table 2 Analytical results on sphalerites from 14 studied mines.

No.	Name of mine	Number of analyzed points	FeS (mol%) Mean	S.D.	Range	MnS (mol%) Mean	S.D.	Range	CdS (mol%) Mean	S.D.	Range	Remarks
1	Buyong	17	13.18	2.940	8.39-16.92	0.33	0.087	0.15-0.48	0.39	0.186	0.15-0.79	m
2	Sihung	85	14.34	3.302	6.43-23.25	0.53	0.465	0.02-2.02	0.47	0.151	0.16-0.77	c
3	Sinyemi	148	13.79	5.188	5.10-25.6	1.48	0.893	0.34-4.55	0.21	0.083	0.05-0.56	c
4	Sangdong	290	16.50	1.544	12.85-20.46	0.46	0.310	0.00-1.10	2.14	0.477	0.94-2.80	m
5	Geodo	7	14.04	1.715	11.16-15.31	0.10	0.102	0.02-0.30	0.31	0.161	0.15-0.45	P
6	No. 1 Yeonhwa	80	21.39	2.280	17.27-28.52	1.39	0.678	0.49-3.04	0.39	0.064	0.24-0.53	m
7	No. 2 Yeonhwa	82	19.60	2.112	13.03-24.75	1.79	0.675	0.64-3.56	0.36	0.057	0.20-0.49	m
8	Ulchin	51	20.42	2.710	10.88-24.37	2.07	1.386	0.18-6.86	0.38	0.126	0.01-0.53	m
9	Susan	61	14.90	6.243	4.09-22.55	1.37	0.937	0.27-3.25	0.91	0.191	0.39-1.17	m
10	Wolag	147	13.27	4.083	5.92-19.51	0.46	0.378	0.00-1.29	0.87	0.318	0.42-1.47	m, p
11	Ulsan	73	19.14	1.613	15.81-23.32	0.27	0.151	0.03-0.82	0.29	0.074	0.12-0.52	m
12	Ilgwang	70	19.93	3.008	14.41-23.26	0.23	0.232	0.00-0.62	0.53	0.089	0.35-0.77	P
13	Mulgum	15	9.88	1.790	7.82-15.47	0.65	0.135	0.40-0.85	0.16	0.049	0.11-0.26	P
14	Haman	47	6.22	2.472	4.74-15.77	0.09	0.047	0.00-0.17	0.35	0.054	0.23-0.49	P

S.D.: standard deviation

Remarks: Used specimens for preparation of polished sections; m: concentrates (mill products), c: composite polished sections prepared by several crushed hand specimens, p: normal polished sections.

(Fe-W) mines were obtained from such specimens.

The second one is prepared from several crushed hand specimens which were collected from the different sites of the deposits. In the case of the Sinyemi (Zn-Pb-Mo) and Sihung (Pb-Zn-Cu) mines, this type of polished sections was used and described as composite polished sections in Table 2.

The third one is a normal polished section made from a hand specimen. It was very difficult to identify sphalerite megascopically in the hand specimens collected from the Geodo (Fe-Cu), Mulgum (Fe) and Haman (Cu) mines. Then several polished sections were checked under the microscope for each deposit.

Composition of sphalerite was determined by an electron probe microanalyzer of JXA-5, JEOL with 40° take-off angle at the Geological Institute, University of Tokyo. Three elements, iron, manganese and cadmium were measured by a partial analysis method. Zinc and sulfur contents of sphalerite were calculated assuming that the atomic proportion of metals including zinc, iron, manganese and

cadmium to sulfur is 1:1. The accelerating voltage was 25 kV, and used standards were natural chalcopyrite of known composition for iron, synthetic MnS for manganese, and synthetic CdS for cadmium. High and low background counts for each element were measured on metallic molybdenum and aluminum, respectively. The X-ray intensities at each point were measured only one time for a fixed interval of 10 seconds. Quantitative corrections of the intensity data for the atomic number, absorption and fluorescence effects were performed by using the computer program FEMAC for the partial analysis of sphalerite, which was modified from the method proposed by Sweatman and Long (1969).

Result and Discussion

The iron, manganese and cadmium contents in sphalerites determined by the electron probe microanalyzer were recalculated to FeS, MnS and CdS mole percent. Arithmetic mean, standard deviation and range of contents of each component are listed in Table 2. The number of the analyzed points for the
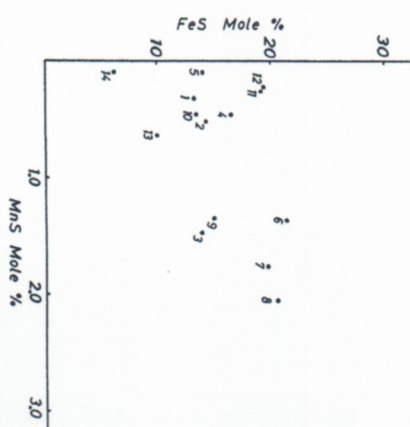
Fig. 1 The relation between mean FeS and MnS contents of the studied sphalerites. Numbers correspond to those of the mines listed in Tables 1 and 2.
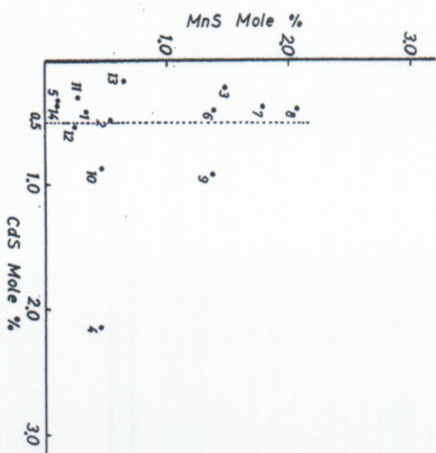
Fig. 2 The relation between mean MnS and CdS contents of the studied sphalerites. Dotted line means the average value of CdS mole% in sphalerites (~0.5 mole%) suggested by MOOKHERJEE (1962). The numbers correspond to those of the mines listed in Tables 1 and 2.

sphalerite are identified under the microscope.

FeS contents of sphalerites from the deposits where pyrrhotite is rare or absent, are less than 20 mole percent. Those deposits include Bupyong, Geodo, Mulgum and Haman (SHIMAZAKI, SATO and CHON, 1981b). In the other ten deposits, pyrrhotite with or without pyrite is common, and FeS contents of sphalerites from those deposits show reasonably large variations. The mean contents of FeS and MnS are plotted together in Figure 1. Relatively MnS-rich sphalerites are also enriched in FeS molecules, but the reverse relation is not always the case.

The relation between MnS and CdS contents of sphalerites is shown in Figure 2. About 0.5 mole percent of CdS was suggested as an average value in sphalerites from various types of hydrothermal ore deposits (MOOKHERJEE, 1962; SHIMAZAKI and SHIMIZU, 1980). Dotted line in Figure 2 shows this average CdS content of hydrothermal sphalerites. The composition of sphalerites from the Sinyemi, No. 1 and No. 2 Yeonhwa and Ulchin mines (Nos. 3, 6, 7 and 8 in the figure), important Zn-Pb producers in Korea, is characterized by high MnS and low CdS content (less than 0.5 CdS mole percent). On the contrary, sphalerites from tungsten deposits such as the Sangdong, Wolag and Ilgwang mines (Nos. 4, 10 and 12 in Fig. 2), belong to another group of low MnS and high CdS mole percent. High MnS content is exceptionally observed in sphalerites from the Susan tungsten-manganese mine (No. 9 in the figure). Third group includes iron and/or copper deposits such as the Geodo, Mulgum and Haman mines (Nos. 5, 13 and 14 in the figure), which are characterized by sphalerites of low MnS and CdS content.

It is worthy of note that the variation of sphalerite compositions is almost similar among similar type of ore deposits. For example, sphalerites from the No. 1 and No. 2 Yeonhwa and Ulchin mines are the case as shown in Figure 3. These three zinc-lead mines are spatially close to each other, and are thought to have genetical relation to similar hypabyssal igneous rocks (Table 1). Mean FeS and CdS
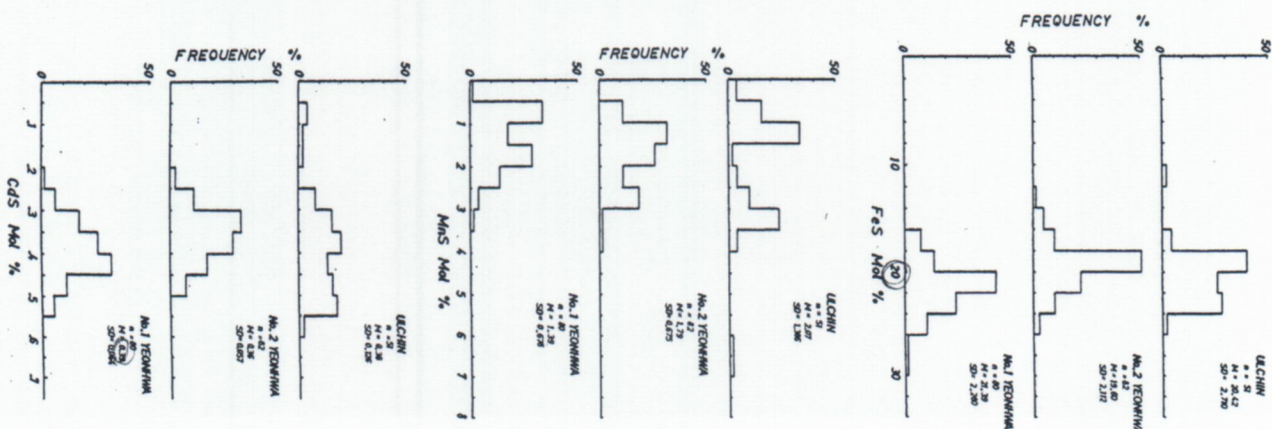
Bupyong, Geodo, Mulgum and Haman deposits are less than 50, because only small sphalerite inclusions in other sulfide minerals, especially in chalcopyrite, or a few grains of

Fig. 3 Frequency distribution of FeS, MnS and CdS mole% in sphalerites from the No. 1 and No. 2 Yeonhwa and Ulchin mines. n: number of analyzed data, M: mean value of analyzed point, SD: standard deviation.

contents are about 20 and 0.4 mole percent, respectively. Compared with other mines, MnS contents are so high ranging from 1.39 to 2.07 mole percent in mean values. Such results correspond to the abundance of manganese minerals in skarns of these deposits.

Further an interesting trend is observed in the Wolag tungsten mine as shown in Figure 4. There are two main veins in the mine which were formed apparently under the same geologic settings (Table 1). Sulfide minerals such as chalcopyrite, galena and arsenopyrite are abundant in Kwangchon veins, while wolframite, molybdenite, pyrite, pyrrhotite and scheelite are predominant in Dongan veins. Among the three components in sphalerites, CdS shows the most sensitive variation in relation to the associated ore minerals. In other words, the CdS content of sphalerites seems to be remarkably related to the abundance of tungsten minerals even under the almost same geologic environments of ore formation.

All tungsten ore deposits studied in the present paper are genetically related to plutonic rocks, and display high CdS content of sphalerites without exception, ranging up to 2.80 mole percent CdS in the Sangdong mine. The reason why cadmium is enriched in sphalerites in tungsten ore deposits is not yet solved physicochemically. Similar compositional variation of sphalerites is also recognized in sphalerites from some Japanese hydrothermal ore deposits (SHIMAZAKI and SHIMIZU, 1980), and will remain to be solved in the future.

electron probe microanalyzer was greatly appreciated. By courtesy of Professor J. Toshimichi Iiyama, this study was possible at the above Institute, where he worked as a visiting researcher from May to December in 1980. The study was carried out as a part of an overseas expedition financially supported by the Ministry of Education of Japan. They are much indebted to Professor Akio Tsusue of the Kumamoto University for the organization of this expedition.

References

Barton, P. B. Jr. and Toulmin, P., 3rd (1966): Phase relations involving sphalerite in the Fe-Zn-S system. Econ. Geol., 61, 815~849.

Fleischer, M. (1955): Minor elements in some sulfide minerals. Econ. Geol., 50th Ann. Vol, 2, 970~1024.

Mookherjee, A. (1962): Certain aspects of the geochemistry of cadmium. Geochim. Cosmochim. Acta, 26, 351~360.

Scott, S. D. and Barnes, H. L. (1971): Sphalerite geothermometry and geobarometry. Econ. Geol., 66, 653~669.

Shimazaki, H., Sato, K. and Chon, H. T. (1981a): Mineralization associated with Mesozoic felsic magmatism in Japan and Korea. Mining Geol. 31, 297~310.

Shimazaki, H., Sato K. and Chon H. T. (1981b): Metallic mineralization associated with Mesozoic granitic magmatism in Korea. In Tsusue, A. (ed.): Petrographic provinces of granitoids and associated metallic ore deposits in the south Korean peninsula, 161 p. 125~153.

Shimazaki, H. and Shimizu, M. (1980): Contents of FeS, MnS and CdS in sphalerites from skarn-type ore deposits in Japan. In Yamaoka, K. (ed.): Abstracts for 2nd Symposium on Genesis of Metallic Mineral Deposits of Granitic Affinity, 10~15 (in Japanese).

So, C. S. (1977): Spurenelement-Paragenese in Zinkblenden verschiedener Pb-Zn-Vorkommen in Korea. Mineral. J. (Japan), 8, 439~455.

Sweatman, T. R. and Long J. V. P. (1969): Quantitative electron microprobe analysis of rock forming minerals. J. Petrol., 10, 332~379.

Takahashi K. (1963): Geochemical study on minor elements in sulfide minerals. Rept. Geol. Survey Japan, 199, 1~69 (in Japanese).

Williams, K. L. (1967): Electron probe microanalysis of sphalerite. Amer. Mineral., 52, 1740~1747.

Fig. 4 Frequency distribution of FeS, MnS and CdS mole% in sphalerites from two main veins of the Wolag mine. See Fig. 3 for explanation of n, M and SD.

indebted greatly to Professor Min Sung Lee of College of Education of the above University, and Dr. Sahng Yup Kim of the Korea Institute of Energy and Resources for their continuous help and advice. Kind help by Messrs. Satoru Nakashima, Masaaki Shimizu and other graduate students of the Geological Institute, University of Tokyo, for the operation of the

大韓民国における熱水性金属鉱床の
閃亜鉛鉱の化学組成変化

全 李謨・島崎英彦・佐藤興平

要旨: 韓国における14の熱水性鉱床の閃亜鉛鉱について, 低い CdS 含有量で特徴づけられるが, タングステン鉱床の閃亜鉛鉱は, 比較的 MnS に富む閃亜鉛鉱は, FeS の含有量も その FeS, MnS, CdS 含有量を X 線マイクロアナライザーにより測定した. 結果は第2表にX線イクロナで, また比較的低い CdS 含有量を示す. 鉛および床型閃亜鉛鉱床では高い CdS 含有量を示す. 鉛および第2表に示すとおりで, また比較的高い MnS と CdS の含有量はある. 比較的低い MnS とともに低い特徴がある. 亜鉛-鉛-銀鉱床産の閃亜鉛鉱は高い MnS と共に低い特徴がある.